Supporting Information
SI Appendix

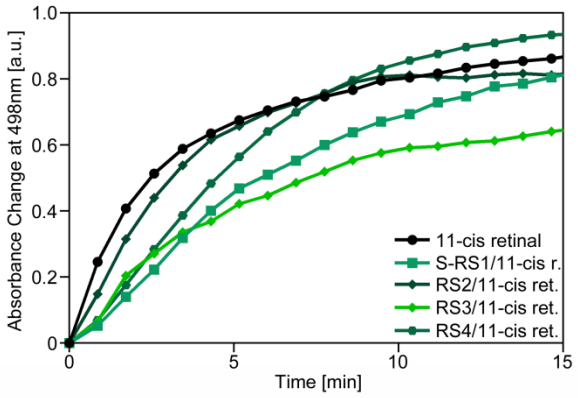

Fig. S1. Regeneration of rhodopsin pigment in the presence of RS1-4. Absorbance changes measured at by UV/VIS at 498 nm indicate the formation of a stable 11-cis retinal-opsin complex (rhodopsin) after mixing 20 µM 11-cis retinal and bovine rod outer segment disc membranes containing 3 µM opsin.. Membranes were premixed with no or 120 µM compound S-RS1 or RS2-4 and incubated for 30 minutes at 20 °C in a buffer containing 60 mM phosphate buffer pH 6.5 with 0.01 % (w/v) n-decyl-β-D-maltopyranoside. Half-time values for pigment formation were determined by background subtraction and one-phase association fit in Graph Pad Prism (not shown) yielding 3 min for 11-cis retinal, 6.2 min for RS1, 7.6 min for RS2, 3.8 min for RS3 and 4 min for RS4, respectively. The presence of S-RS1 and RS2 thus resulted in significantly reduced rates of pigment formation indicative for binding in the orthosteric binding pocket. Notably, none of the compounds prevented formation of stable rhodopsin pigment.

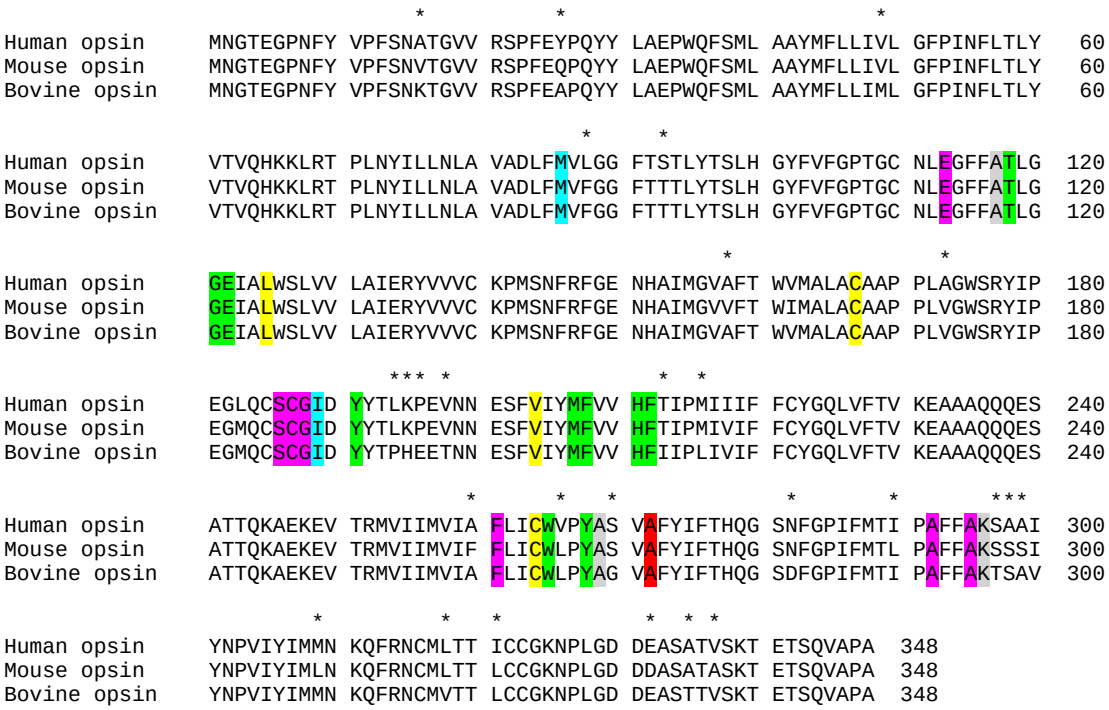

Fig. S2. Multiple sequence alignment of human, mouse and bovine rhodopsin highlighting residues involved in S-RS1 binding. Human opsin has a sequence identity of 93.4 % and 94.8 % to bovine and mouse opsin, respectively. Non-conserved residues are marked with asterisks. Colored residues identify interaction sites within a distance of 4.5 Å of three ligands 11-*cis* retinal (grey), all-*trans* retinal and the S-RS1 (green), of 11-*cis* retinal and all-*trans* retinal (grey) but not S-RS1, of all-*trans* retinal and the S-RS1 (red), of 11-*cis* retinal alone (pink), with all-*trans* retinal alone (cyan) and with S-RS1 alone (yellow).

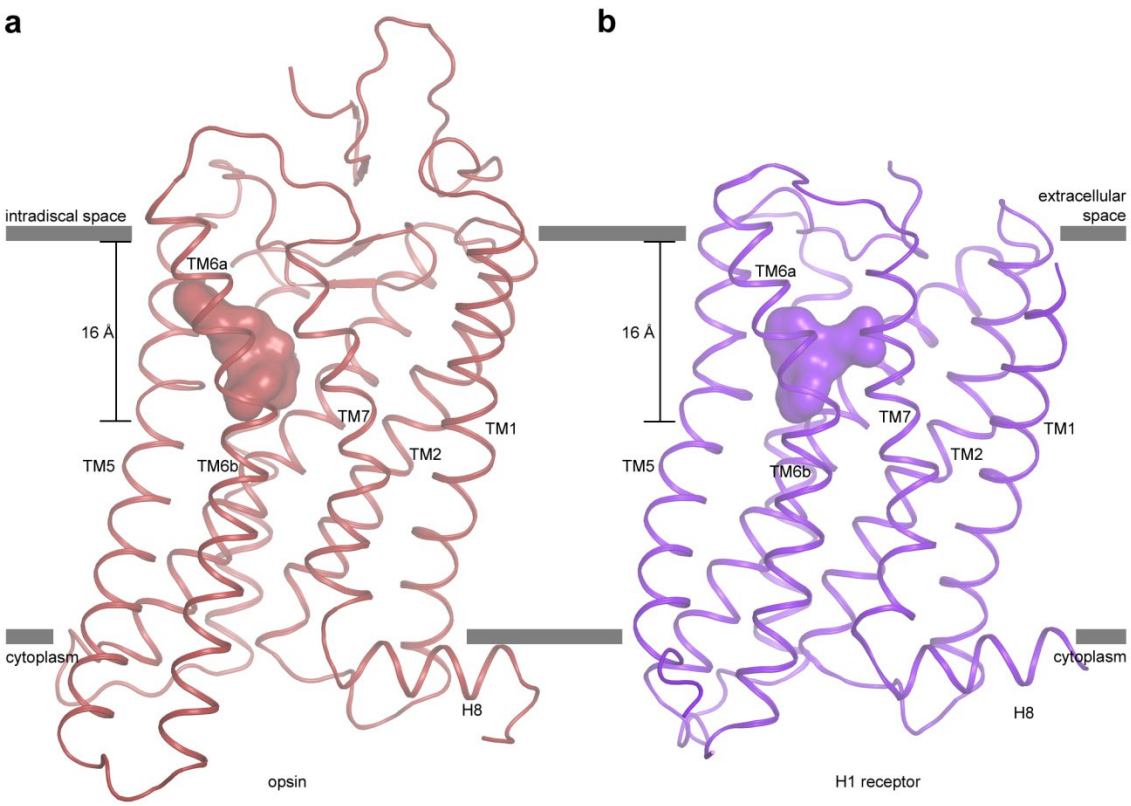

Fig. S3: Comparison of the ligand binding sites of opsin and histamine H_1 receptor. Side view and cartoon representation of **a,** S-RS1-bound opsin **b,** doxepin-bound histamine H_1 receptor (PDB ID: 3RZE) showing the ligands in surface representation. Bars indicate depth measurements using Pymol from the upper end of TM6a and the lower end of the ligand.

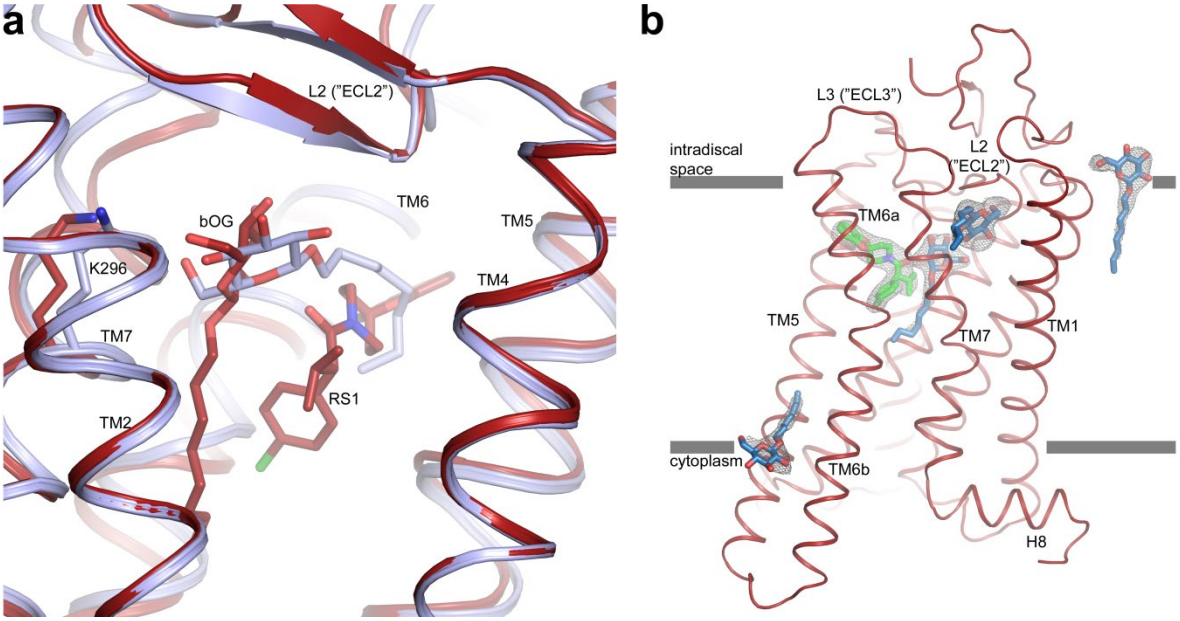

Fig. S4: Octylglucoside binding sites in S-RS1-bound opsin. a, superposition of S-RS1-bound and retinal-free, detergent-bound opsin (PDB ID: 4J4Q) showing overlapping sugar moieties but turned alkyl chains by an angle of 90°. TM3 has been removed for clarity. **b,** Side view of the S-RS1-opsin complex in cartoon representation showing S-RS1 and all four modelled β-octyl glucoside molecules in green and blue sticks, respectively. Experimental electron density (F_o-F_c) maps (gray mesh) are contoured at 3 σ. The inner surface area of the binding pocket is considerably expanded to 1520 $Å^2$ compared to 599 $Å^2$ and 603 $Å^2$ for dark and metaII state rhodopsin, respectively.

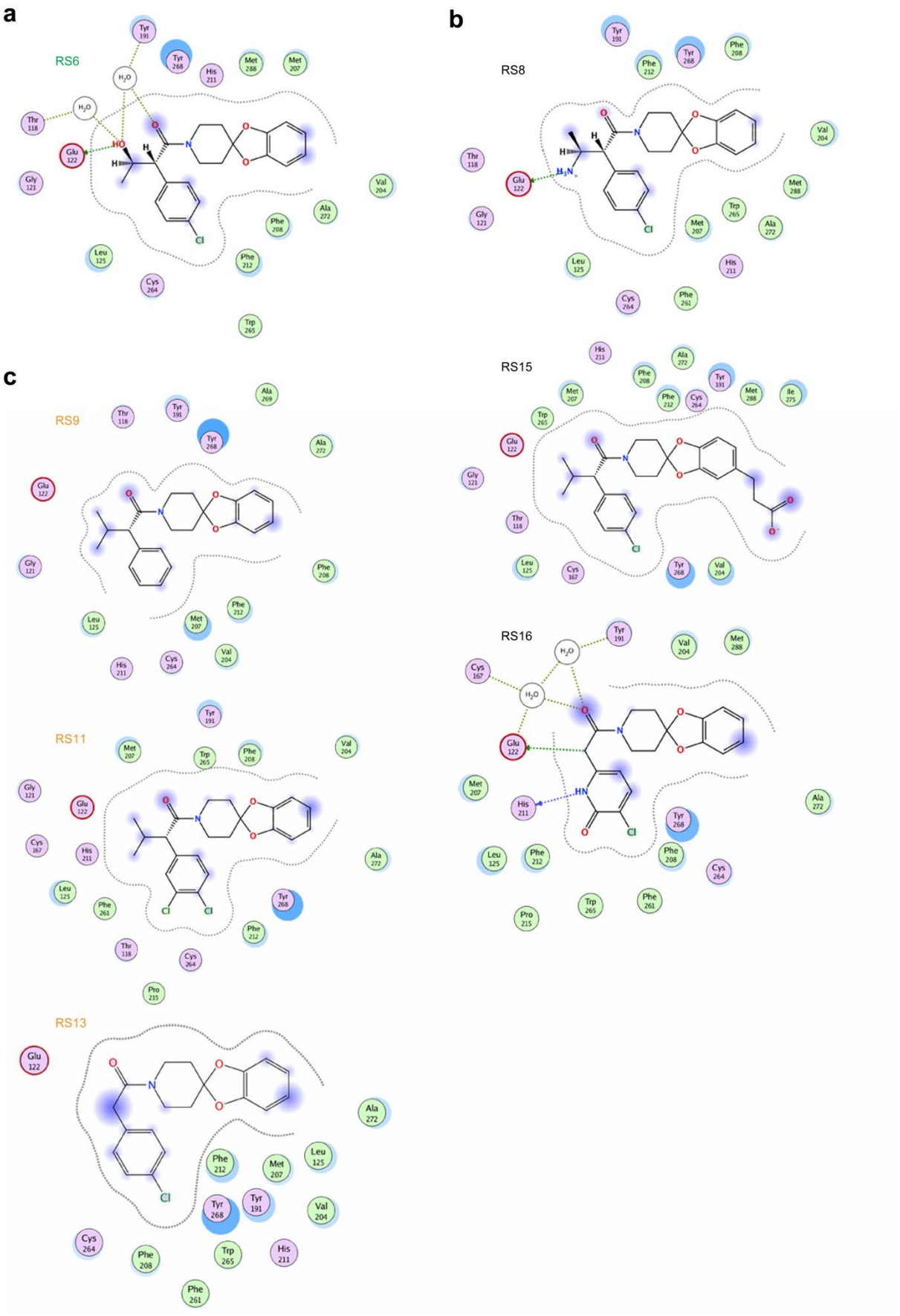

Fig. S5: MOE calculated protein-ligand schematic based on crystal structures of the S-RS1 derivatives. a-c, The color code for S-RS1 derivative names follows the groups

identified for limited chemical modification as in shown in Fig 3. Key interactions between S-RS1 derivatives and opsin detailing hydrophilic residues (purple), basic groups (blue rings), acidic groups (red rings), hydrophobic residues (green), hydrogen bonds (arrows) and blue discs on ligand atoms indicate solvent exposure when bound, light blue shadows indicate contact surface area.

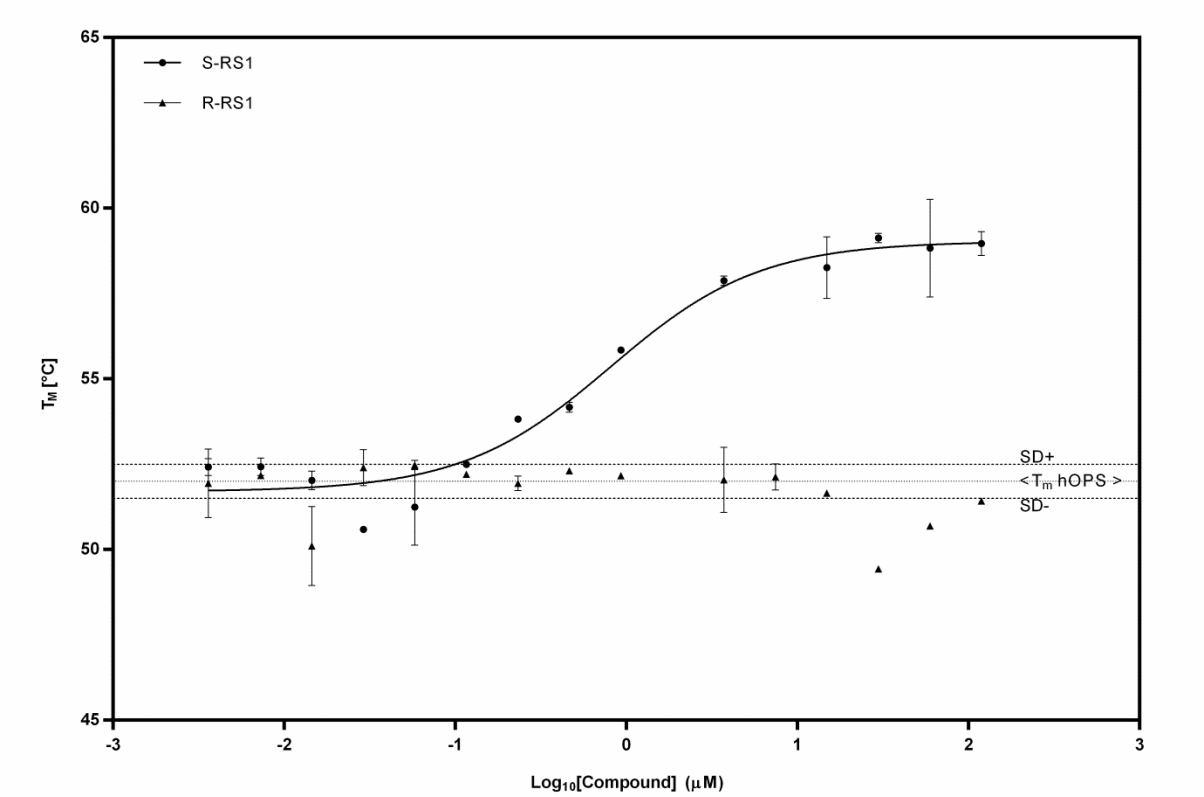

Fig. S6: Dose-response thermofluor assay of S- and R-RS1. 14-point titration at 0.004 µM, 0.007 µM, 0.015 µM, 0.029 µM, 0.058 µM, 0.116 µM, 0.233 µM, 0.465 µM, 0.930 µM, 3.720 µM, 14.881 µM, 29.762 µM, 59.524 µM and 119.048 µM using 1.3 µM human opsin N2C N282C. An EC_{50} value of 0.8 µM is determined for the S enatiomer. Rather than binding, we observe a destabilizing effect for human opsin for the R-RS1 at concentrations above 15 µM. All data points were measured in triplicates and the data is shown as mean ± S.D..

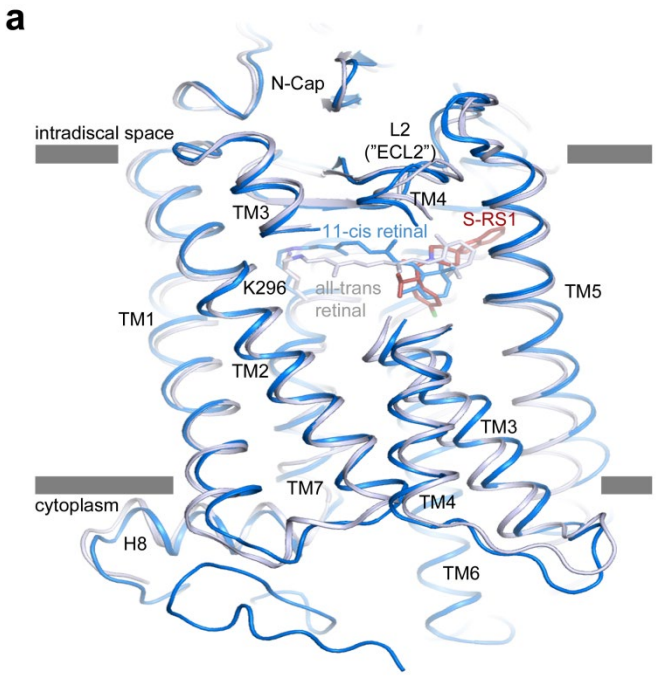

Fig. S7: Comparison of S-RS1-, all-trans retinal- and 11-cis retinal-binding to opsin. Side view of superimposed dark state (blue; PDB ID: 1GZM), meta-II active state rhodopsin (bluewhite; PDB ID: 3PQR) and S-RS1-bound opsin (red, opsin structure omitted, only S-RS1 shown). The β-ionone ring of the agonist all-trans retinal (dark state conformation, bluewhite) overlaps with the chlorinated phenyl ring of S-RS1 (red), whereas the β-ionone ring of the inverse agonist 11-cis retinal (metaII active conformation, blue) overlaps with the location of the spiro group of S-RS1. S-RS1 stabilizes the novel conformation by addressing locations known to be critical to generate retinal-bound dark state or metaII active conformations.

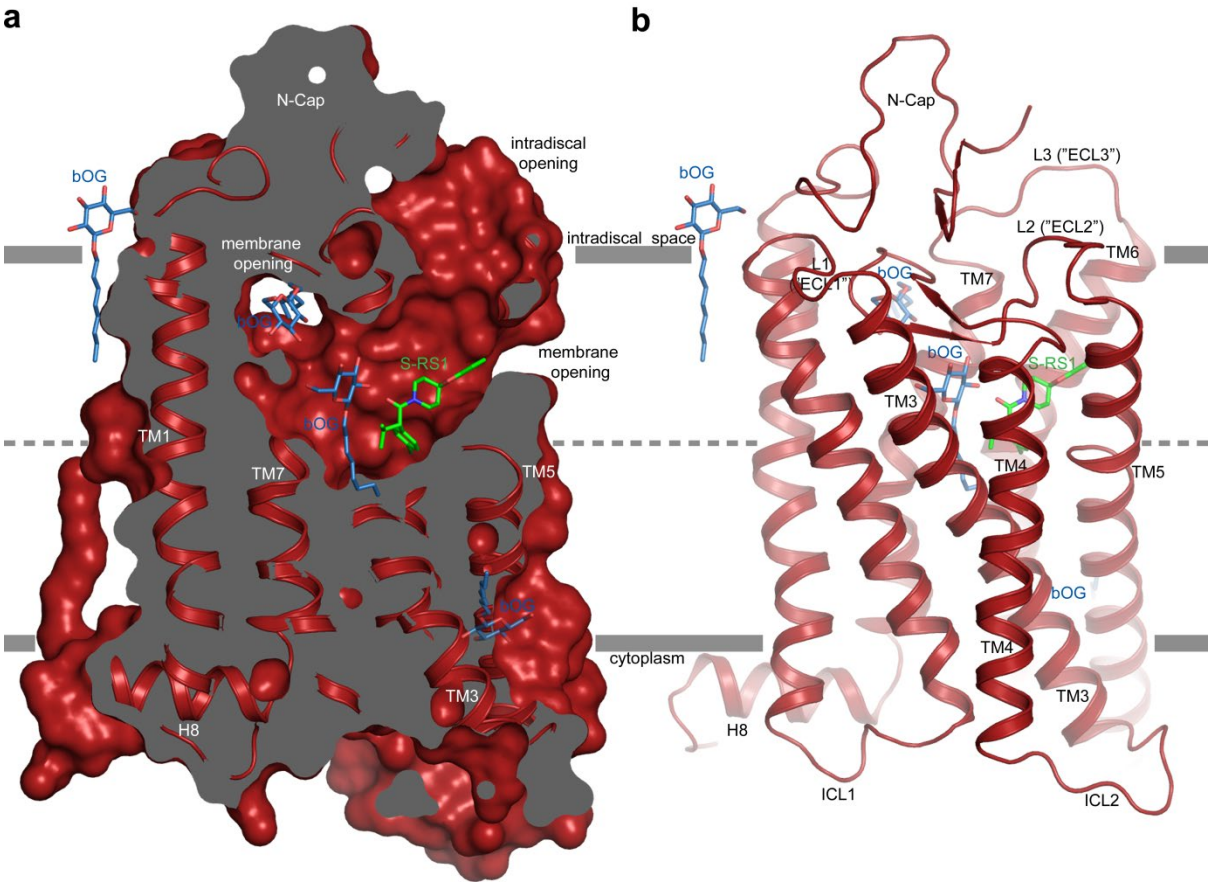

Fig. S8: Side view of a ligand channel in S-RS1-stabilized opsin. a, Combined surface and cartoon representation of the S-RS1-octylglucoside-opsin complex sliced perpendicular to the membrane. The view highlights an intradiscal opening formed between L2 ("ECL2"), TM5 and TM6a as well as an opening towards the membrane providing enough space for the exchange of hydrophobic molecules. Overlayed S-RS1 and octylglucoside molecules indicate locations rather than exact positions or slice. **b,** S-RS1-octylglucoside-opsin complex in cartoon representation in the non-sliced, analogous view of **a** to visualize exact S-RS1 and octylglucoside positions and clearly assignable transmembrane helices.

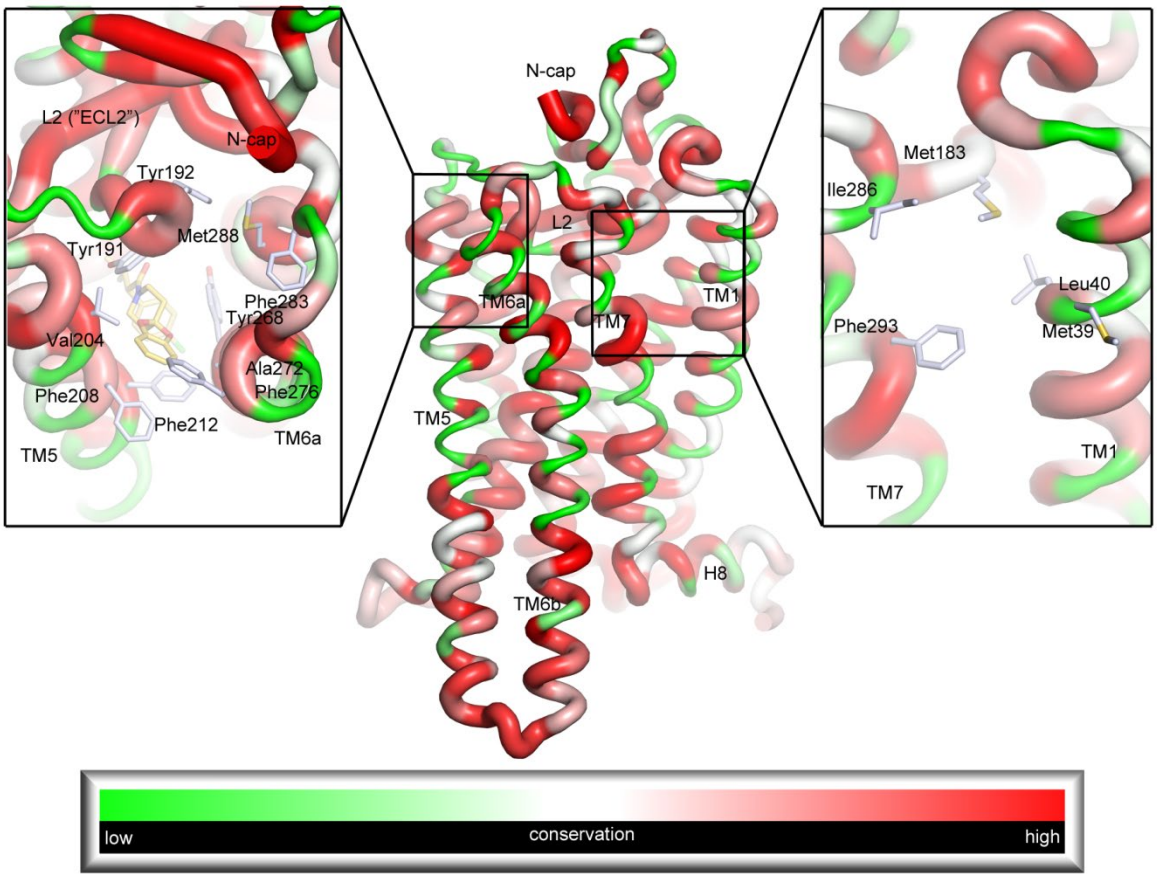

Fig. S9: Structural alignment of 96 vertebrate opsin sequences and structural visualizing of the amino acid conservation. Cartoon representation of the S-RS1-opsin complex showing residues of low conservation using thin green, and a high conservation in thick red lines. Sequences exhibit a very high sequence similarity as shown by color intensity (color intensity panel). Residues along the intradiscal opening shaped by L2 ("ECL2"), TM5 and TM6a are highly conserved (left panel close-up), whereas the level of conservation appears to be lower for the membrane opening between TM7/TM1 suggesting kinetic influences for ligand entry or exit (right panel close-up). Residues important for the retinal uptake and release are highlighted in stick.

Table S1: Data collection and refinement statistics for S-RS1

Data collection	
Space group	$R3_2$
Cell dimensions	
a,b,c (Å)	244.2, 244.2, 111.8
α,β,γ (°)	90, 90, 120
Resolution (Å)[a]	46.15 - 2.36 (2.444 - 2.36)
R_{merge}	0.1141 (5.21)
I/σI	16.49 (0.56)
$CC_{1/2}$	0.999 (0.264)
Completeness (%)	100 (100)
Redundancy	11.4 (11.9)

Refinement	
Resolution (Å)	46.15 - 2.36 (2.444 - 2.36)
No. reflections	52045
R_{work}/R_{free}	0.2164/0.2261
No. atoms	
Protein	2616
Ligand/detergents	171
Water	79
B-factors (Å^2)	
Protein	85.39
Ligand/detergent	98.03
Water	88.63
R.M.S.D.	
Bond lengths (Å)	0.004
Bond angles (°)	0.77
Ramachandran statistics[b] (%)	
Favored	96
Allowed	4
Outliers	0

[a]Values in parentheses are for the highest resolution shell. [b]As calculated by MolProbity

Table S2. List of opsin-ligand interactions including distance values.

Amino acid	Ligand	Distance (Å)	Interaction type
Met86	b-OG	4.374	distance
Met86	all-*trans* retinal	4.31	distance
Glu113	*11-cis* retinal	4.162	distance
Ala117	b-OG	3.962	distance
Ala117	11-*cis* retinal	3.791	distance
Ala117	all-*trans* retinal	3.812	distance
Thr118	b-OG	4.253	distance
Thr118	S-RS1	3.968	distance
Thr118	11-*cis* retinal	4.109	distance
Thr118	all-*trans* retinal	3.979	distance
Gly121	b-OG	4.081	distance
Gly121	S-RS1	3.853	distance
Gly121	11-*cis* retinal	3.815	distance
Gly121	all-*trans* retinal	4.482	distance
Glu122	S-RS1	3.911	distance
Glu122	11-*cis* retinal	4.099	distance
Glu122	all-*trans* retinal	4.008	distance
Ala124	b-OG	4.278	distance
Leu125	b-OG	4.383	distance
Leu125	S-RS1	4.04	distance
Leu128	b-OG	3.771	distance
Cys167	S-RS1	4.348	distance
Glu181	b-OG	3.988	distance
Ser186	11-*cis* retinal	4.185	distance
Cys187	b-OG	4.212	distance
Cys187	11-*cis* retinal	3.666	distance
Gly188	b-OG	3.814	hydrogen bonding
Gly188	11-cis retinal	4.017	distance
Ile189	b-OG	3.971	distance
Ile189	11-*cis* retinal	3.835	distance
Ile189	all-*trans* retinal	4.436	distance
Tyr191	S-RS1	4.045	distance
Tyr191	11-cis retinal	4.014	distance
Tyr191	all-trans retinal	4.185	distance
Tyr192	b-OG	4.312	distance
Val204	S-RS1	3.892	distance
Met207	S-RS1	4.079	distance
Met207	11-*cis* retinal	3.942	distance
Met207	all-*trans* retinal	4.184	distance
Phe208	S-RS1	4.068	distance
Phe208	11-*cis* retinal	4.272	distance
Phe208	all-trans retinal	4.129	distance
His211	S-RS1	3.977	distance
His211	11-*cis* retinal	4.253	distance
His211	all-*trans* retinal	3.843	distance
Phe212	S-RS1	4.209	distance
Phe212	11-*cis* retinal	3.807	distance
Phe212	all-*trans* retinal	4.234	distance
Phe261	b-OG	3.789	distance
Phe261	11-*cis* retinal	4.111	distance

Cys264	b-OG	4.103	distance
Cys264	S-RS1	4.126	distance
Trp265	S-RS1	3.957	distance
Trp265	11-*cis* retinal	4.136	distance
Trp265	all-*trans* retinal	4.169	distance
Tyr268	b-OG	3.661	distance
Tyr268	S-RS1	4.06	distance
Tyr268	11-*cis* retinal	4.063	distance
Tyr268	all-*trans* retinal	4.11	distance
Ala269	11-*cis* retinal	4.247	distance
Ala269	all-*trans* retinal	4.114	distance
Ala272	S-RS1	3.519	distance
Ala272	all-*trans* retinal	3.939	distance
Ala292	b-OG	3.975	distance
Ala292	11-*cis* retinal	4.061	distance
Ala295	b-OG	4.215	distance
Ala295	11-*cis* retinal	4.353	distance
Lys296	b-OG	3.963	distance
Lys296	11-*cis* retinal	3.228	covalent binding
Lys296	all-*trans* retinal	3.22	covalent binding
Ser298	b-OG	4.029	distance
Asn302	b-OG	3.984	distance

Table S3. Data collection and refinement statistics.

	RS15	RS6	RS9	RS8	RS13	RS11	RS16
Data collection							
Space group	$R3_2$	$R3_2$	$R3_2$	$R3_2$	$R3_2$	$R3_2$	$R3_2$
Cell dimensions							
a,b,c (Å)	243.2, 243.2, 111.9	243.4, 243.4, 111.5	243.2, 243.2, 111.7	242.2, 242.2, 111.0	242.9, 242.9, 111.5	244.1, 244.1, 111.2	243.4, 243.4, 111.8
α,β,γ (°)	90, 90, 120	90, 90, 120	90, 90, 120	90, 90, 120	90, 90, 120	90, 90, 120	90, 90, 120
Resolution (Å)[a]	49.4 - 2.46	47.65 - 2.62	47.63 - 2.63	45.77 - 2.87	45.89 - 3.03	47.74 - 2.46	45.76 - 2.49
	(2.548 - 2.46)	(2.714 - 2.62)	(2.724 - 2.63)	(2.973 - 2.87)	(3.138 - 3.03)	(2.548 - 2.46)	(2.579 - 2.49)
R_{merge}	0.1194 (3.204)	0.2588 (4.444)	0.1679 (3.96)	0.1926 (3.531)	0.3432 (4.311)	0.107 (3.089)	0.1527 (3.037)
I/σI	16.96 (0.84)	10.97 (0.69)	13.87 (0.53)	12.28 (0.72)	8.98 (0.70)	17.46 (0.65)	13.83 (0.78)
$CC_{1/2}$	1 (0.41)	0.998 (0.288)	0.999 (0.332)	0.999 (0.407)	0.997 (0.32)	1 (0.364)	0.999 (0.389)
Completeness (%)	1.00 (1.00)	1.00 (1.00)	1.00 (1.00)	1.00 (1.00)	1.00 (1.00)	1.00 (1.00)	1.00 (0.99)
Redundancy	11.5 (11.1)	11.5 (11.9)	11.5 (11.9)	11.5 (11.5)	11.3 (11.8)	11.5 (11.1)	11.5 (11.6)
Refinement							
Resolution (Å)	49.4 - 2.46	47.65 - 2.62	47.63 - 2.63	45.77 - 2.87	45.89 - 3.03	47.74 - 2.46	45.76 - 2.49
	(2.548 - 2.46)	(2.714 - 2.62)	(2.724 - 2.63)	(2.973 - 2.87)	(3.138 - 3.03)	(2.548 - 2.46)	(2.579 - 2.49)
No. reflections	45696	37795	37419	28425	24405	45781	44047
R_{work}/R_{free}	0.2315/0.2455	0.2361/0.2525	0.2348/0.2607	0.2415/0.2609	0.2541/0.2688	0.2129/0.2234	0.2345/0.2582
No. of atoms	2835	2824	2789	2687	2806	2821	2805
Protein	2605	2605	2616	2556	2619	2605	2616
Ligands/detergent	196	191	170	131	187	192	189
Waters	34	28	3	-	-	24	-
B-factors							
Protein	71.95	75.72	90.64	94.75	90.39	81.51	78.22
Ligands/detergent	85.24	88.65	110.72	120.42	110.06	96.73	97.15
Water	60.85	65.84	68.52	-	-	67.28	-
R.M.S.D.							
Bond length (Å)	0.004	0.004	0.004	0.003	0.005	0.009	0.007
Bond angles (°)	0.73	0.64	0.70	0.66	1.03	0.94	0.92
Ramachandran statistics[b] (%)							
Favored	95	97	97	93	93	96	96
Allowed	4	3.1	2.8	7	5.6	3.4	3.7
Outliers	0.62	0	0	0	1.5	0.62	0.62

[a]Values in parentheses are for the highest resolution shell. [b]As calculated by MolProbity

Table S4. Small molecule data collection and refinement statistics.

Identification code	**RS1 (R-enantiomer)**	**RS1 (S-enantiomer)**
Empirical formula	$C_{22}H_{24}ClNO_3$	$C_{22}H_{24}ClNO_3$
Formula weight	385.87	385.87
Temperature/K	130(2)	130(2)
Crystal system	Monoclinic	Monoclinic
Space group	$P2_1$	$P2_1$
a/Å	9.9129(3)	9.9099(3)
b/Å	10.3507(2)	10.3432(3)
c/Å	19.5371(4)	19.5532(7)
α/°	90.00	90.00
β/°	93.273(2)	93.281(3)
γ/°	90.00	90.00
Volume/Å^3	2001.34(8)	2000.92(11)
Z	4	4
ρ_{calc}/ g/cm^3	1.281	1.281
Absorption coefficient/μ/mm^{-1}	1.862	1.863
F(000)	816	816
Crystal size/mm^3	0.500 x 0.500 x 0.400	0.200 x 0.150 x 0.080
2Θ range for data collection/°	4.467 to 63.551	4.469 to 63.569
Index ranges	$-11 \le h \le 11$, $-12 \le k \le 12$, $-22 \le l \le 22$	$-11 \le h \le 11$, $-12 \le k \le 12$, $-22 \le l \le 22$
Reflections collected	64131	33173
Independent reflections	6567 [R_{int} = 0.0494]	6580 [R_{int} = 0.0628]
Data/restraints/parameters	6567/1/679	6580/1/679
Goodness-of-fit on F^2	1.036	1.023
Final R indexes [I>=2σ (I)]	R_1 = 0.0247, wR_2 = 0.0617	R_1 = 0.0333, wR_2 = 0.0702
Final R indexes [all data]	R_1 = 0.0251, wR_2 = 0.0612	R_1 = 0.0478, wR_2 = 0.0734
Largest diff. peak/hole / e Å^{-3}	0.148/ -0.244	0.156/-0.229

SI Experimental Procedures

Selection of focused library

Five complementary in silico methods were used to compile the focused library screened in this study. All-*trans* retinal served as the reference molecule for a 2D ligand similarity search in the Roche compound library using Pipeline Pilot ECFP6 fingerprints (1). In addition, three published non-covalent opsin binders (2, 3) were used as templates for similarity searches using the graph-based Maximum Overlapping Set (MOS) approach available in Spinifex and 3D shape matching as implemented in ROCS (4, 5). The 3D coordinates for reference molecules were generated with the Moloc companion program Mol3d using default parameters (6). The crystal structure of rhodopsin with bound all-*trans* retinal (PDB ID: 4A4M) was used as template for a MOE pharmacophore model including five hydrophobic features covering the β-ionone ring and the region close to the ligand head group, as well as excluded volume features for the surrounding protein except for the flexible, retinal-binding Lys296$^{7.43}$ (7). Additional pharmacophore searches were performed with models mimicking a potential covalent interaction with Lys296$^{7.43}$. These were constructed again from the crystal structure of rhodopsin with bound all-*trans* retinal using the same protein excluded volume features as before but combined with pharmacophore features for potential ligand reactive groups. The ligand sub-structures included activated double bonds, activated ketones, aldehydes, nitriles, and sulfonylhalides, which were defined using SMARTS patterns. As a fifth approach, we used GOLD docking (8, 9) with the ChemScore scoring function to both an active (PDB ID: 4A4M) and inactive (PDB ID: 1GZM) conformation of rhodopsin (7, 10). The docking was performed in GOLD library screening mode with an additional hydrogen bonding constraint between any ligand atom and NZ of Lys296$^{7.43}$. The residue was allowed to relax during docking. Top-ranked compounds from each in silico approach were retrieved based on method-specific score thresholds and further pruned in MOE by removing undesired substructures and filtering by the following molecular properties: a) number of heavy atoms: 10-32, b) calculated lipophilicity SlogP >2, c) number of hydrogen bond donors: 0-5. Finally, a chemically diverse subset of the remaining compounds was selected yielding a focused library of 4617 molecules. Whereas the majority of the selections were non-covalent binders, a smaller subset contained compounds with functional groups and the potential to form a covalent interaction with Lys296$^{7.43}$. After screening of this library one round of hit expansion was performed resulting in 5186 molecules tested in total.

Constructs, expression and purification

A detailed description of the cloning, expression, purification and crystallization process can be found here (11). Briefly, full length native human opsin (P08100) stabilized by the functionally neutral disulfide bridge between mutations N2C and N282C (corresponding to N2C/D282C in bovine rhodopsin (12, 13) was subcloned into a tetracycline-inducable pCMV vector for expression in HEK293S GnTI- stable cell lines (14-16). Large scale expression of human opsin was performed in 100 l bioreactors and purified using 1D4 antibody affinity resin (Cubebiotech) by gravity flow. Eluted protein was flash frozen in liquid nitrogen and elution buffer containing 10 mM Hepes-NaOH pH 7.0, 0.125 % (w/v) DM, 80 µM elution peptide (TETSQVAPA) at 5 mg/ml until further use in thermofluor differential scanning fluorimetry (DSF) or fluorescence-detection size-exclusion chromatography thermal shift (FSEC-TS) assays. For crystallization, stabilized bovine opsin N2C/D282C (P02699) was expressed in HEK293S GnTI- stable cell lines and purified. To equilibrate the protein in crystallization buffer containing 10 mM NaOAc-HCl pH 5.0, 100 mM NaCl, 1 % (w/v) b-OG an additional size-exclusion chromatography step was added using a superdex 200 10/300 GL (GE Helthcare).

Crystal soaking, data collection and structure determination of opsin complexes. Crystals were readily obtained using purified bovine opsin N2C/D282C incubated with 0.5-1 times w/w porcine brain polar lipid prior to vapor diffusion sitting or hanging drop

crystallization (11). Crystals were grown over a reservoir solution containing 3.0 to 3.5 M ammonium sulfate, 0.1 M sodium acetate pH 5.75 - 6.0 and 10 % (w/v) trehalose as cryo-protectant. Soaks with 3.75 to 5 mM of compounds were incubated for 24 h prior to flash cooling of crystals with liquid nitrogen. Diffraction data were collected at 100 K on beamline X10SA at the Swiss Light Source. Data sets were integrated using XDS and scaled using SADABS (17). All structures were solved by molecular replacement in Phaser with a rhodopsin search model (PDB ID 4J4Q) (18, 19). Iterative model building was done with Coot followed by refinement in Phenix (20, 21). Caver was used to analyze cavities in the dark state (PDB ID: 1GZM), the meta-II state (PDB ID: 3PQR) and the S-RS1-opsin complex (22-25). Statistics of structure determination are listed in Supplementary Table 1.

Focused screening

A thermofluor assay was adapted and automated to screen the focused library and compounds from hit expansion (26). Briefly, purified human opsin N2C/N282C was diluted to 1.4 µM with assay buffer containing 10 mM HEPES-NaOH pH 7.4, 200 mM NaCl, 0.125 % (w/v) DM, distributed to 72 positions in a 96 well plate and incubated either with 47.6 µM compound or 1.2 % (v/v) DMSO in the first and last position for 30 minutes at room temperature. The total reaction volume was 42 µl. Next, 3 mg/ml N-4-(7-diethylamino-4-metyl-3-coumarinyl)phenyl]malemeide (CPM; Molecular Probes, REFD346) in DMSO (Molecular Probes, REF D12345) was diluted to 0.03 mg/ml in assay buffer. Finally, a concentration of 0.006 mg/ml CPM dye was used to investigate the thermal denaturation of the compound-bound ospin in a total reaction volume of 52 µl[28,29]. Melting curves were obtained applying a temperature gradientfrom 25 to 95 °C and a heating rate of 0.25 °C/s in a Rotor Gene Q (Qiagen). All liquid handling steps were performed using a Bravo Automated Liquid handling platform and a 96LT head (Agilent). Melting temperatures (T_M) were calculated and analyzed by automated scripts using Spotfire (Tibco) and the Boltzmann equation ($Y = T_{min} + \frac{T_{max} - T_{min}}{1 + e^{T_M - x}}$) the minimal and maximal temperatures T_{min} and T_{max}, respectively. Compounds were selected for further characterization based on a stabilizing effect exceeding the threshold of two standard deviations (±2.6 °C) of human opsin N2C/N282C containing DMSO (27). Hits served as reference molecules for a 2D ligand similarity search performed with ECFP6 (1). The hit expansion identified another 569 compounds for screening and characterization.

Hit validation using a fluorescence-detection size-exclusion chromatography thermal shift assay (FSEC-TS)

FSEC-TS served as an orthogonal thermal shift assay to validate the compound-induzed stabilization of human opsin N2C/N282C(28). Each measurement consumed 0.26 µM protein mixed with 10 µM of compound in a final buffer containing 10 mM HEPES- NaOH pH 7.4, 200 mM NaCl, 0.125 % (w/v) DM and 0.1 % (v/v) DMSO and incubated for 30 minutes at 4 °C. Melting temperatureswere determined in duplicate by incubation for 10 minutes in a Prime Thermal cycler (Techne) at 12 different temperaturesbetween 35 °C and 60 °C.Non-aggregated protein was quantified using tryptophan fluorescence after separation on a high-performance liquid chromatography system (Agilent 1200). Melting temperatures (T_m) were determined using the Boltzmann equation fit ($Y = T_{min} + \frac{T_{max} - T_{min}}{1 + e^{T_M - x}}$) with the minimal and maximal temperature T_{min} and T_{max}, respectively. All analysis were performed in GraphPad Prism (GraphPad Software, Inc.).

***Mouse* P23H opsin pharmacotrafficking β-galactosidase complementation assay**

U2OS mouse rhodopsin P23H stable cell lines (DiscoverRx ID 93-1077C3) were used to express a C-terminal fusion of *mouse* opsin P23H with the small β-galactosidase subunit. The large subunit of β-galactosidase was fused to the plasma membrane-expressed pleckstrin homology domain of phospholipase C-δ (29). Cells were cultured in

AssayComplete Cell Culture Media (Cat. No. 92-0018GK3, DiscoverX), grown to approximately 80 % confluency and routinely passages were produced every 2-3 days. A Countess™ automated cell counter (ThermoFisher Scientific) was used to determine the cell density measurements. For final measurements, the cell medium was exchanged to AssayComplete™ CP reagent (Cat. No. 93-0563R5A; DiscoverX). Approximately 5000 cells in a total volume of 40 µl were transferred to each of a well of a 384-well plate and incubated for 4 h at 37 °C in 5 % CO_2. Compounds including the positive control 9-*cis* retinal were added at a final concentration of 5 µM. 4 % (v/v) DMSO served as negative control. Cells were incubated for 20 h at 37 °C in 5 % CO_2 followed by an additional incubation step at room temperature for 3 h before chemiluminescence measurement. Detection was performed with PathHunter Detection Kit reagent (Cat No. 93-0001S, DiscoverX) following the protocol provided by DiscoverX. Chemiluminescence measurements were performed after 1 h of incubation on a BioTek Cytation3 luminescence plate reader. Measurements were evaluated and compared to 9-cis retinal with GraphPad Prism using the normalised dose-response curve, while the lowest value was defined as 0 % and the highest value as 100 % in a compound dataset. All experiments were done under red-light due to the instability of 9-*cis* retinal under normal light conditions.

Compound synthesis and characterization

To perform the macromolecular crystallographic analysis and biophysical characterization of RS1, the racemate was synthesized (Chembiotek, India) and purified to yield the R- and S-enantiomer. Reactions were performed under an atmosphere of argon. Solvents and reagents were obtained from commercial sources and used without further purification. All reactions were monitored by thin-layer chromatography (TLC) on Merck silica gel 60 F254 TLC glass plates (visualized by UV fluorescence at λ = 254 nm). ^{1}H Nuclear Magnetic Resonance (NMR) and ^{13}C NMR spectra were recorded on a Bruker 600 MHz and 150 MHz instrument, respectively. The chemical shifts (δ in ppm) were reported relative to tetramethylsilane as internal standard. Resonances in the ^{1}H NMR spectra were reported to the nearest 0.01 ppm. NMR abbreviations are as follows: s, singlet; d, doublet; t, triplet; q, quadruplet; m, multiplet; br, broad. The purity of final compounds as measured by LC-MS was at least >95 %. Purity of compounds was analyzed by ^{1}H NMR and LC-MS. LC-MS spectra were recorded on a Waters UPLC-MS System equipped with Waters Acquity CTC PAL auto sampler and a Waters SQD single quadrupole mass spectrometer. Analytical separation was conducted on a Zorbax Eclipse Plus C18 2.1 x 30 mm, 1.7 µm column at 50 °C; eluent A = 0.01 % formic acid in water; eluent B = acetonitrile at a flow of 1 mL min-1. Gradient: 0 min 3 % B, 0.2 min 3 % B, 2 min 97 % B, 1.7 min 97 % B and 2.0 min 97 % B. The injection volume was 2 µL. LC-MS high resolution spectra were recorded on an Agilent LC system consisting of an Agilent 1290 high pressure gradient system, a CTC PAL auto sampler and an Agilent 6520 QTOF. Analytical separation was achieved on a Zorbax Eclipse Plus C18 column (2.1 mm x 50 mm, 1.7 µm) at 55 °C; eluent A = 0.01 % formic acid in water; eluent B = 0.01 % formic acid in acetonitrile at a flow of 1 mL min-1. Gradient: 0 min 5 % B, 0.3 min 5 % B, 4.5 min 99 % B and 5 min 99 % B. The injection volume was 2 µL. Ionization was performed in multimode source. The mass spectrometer was run in 2 GHz extended dynamic range mode, resulting in a resolution of about 10 000 at m/z = 922. Mass accuracy was ensured by internal drift correction.

LC/MS (Method A): LC/MS was analyzed on Shimadzu LC / API 2000 (Applied Biosystems) MS instrument in ESI (+/-) ionization mode using Gemini NX C-18 4.6 X 50 mm 5 µ column, Mobile phase: A = 10 mM NH_4OAc buffer & B = CH_3CN, flow 1.2 ml/min. Gradient: 10 % CH_3CN to 20 % CH_3CN in 2.0 min, 20 % to 80 % CH_3CN in next 6 min, 80 % to 100 % CH_3CN in next 2 min. Hold at 100 % CH_3CN for 1.5 min and step down to initial 10 % CH_3CN in 1 min.

(Method B): LC/MS was analyzed on Shimadzu LC / API 2000 (Applied Biosystems) MS instrument in ESI (+/-) ionization mode using Gemini NX C-18 4.6X50 mm 5µ column, Mobile phase: A = 10 mM NH_4OAc buffer & B = CH3CN, flow 1.2 ml/min. Gradient : 10 %

CH_3CN to 30 % CH_3CN in 1.5 min, 30 % to 98 % CH_3CN in next 1.5 min and hold at 98 % CH_3CN for 1.0 min and step down to initial 10 % CH_3CN in 1 min.
(Method C): LC/MS was analyzed on Shimadzu LC / API 2000 (Applied Biosystems) MS instrument in ESI (+/-) ionization mode using Gemini NX C-18 4.6X50 mm 5µ column, Mobile phase: A = 10 mM NH_4OAc buffer & B = CH_3CN, flow 1.0 ml/min. Gradient: Hold at 10 % CH_3CN for 1.0 min, 10 % to 98 % CH_3CN in next 5 min. Hold at 98 % CH_3CN for 6 min and step down to initial 10 % CH_3CN in 1 min.
HPLC Analysis was carried out on Shimadzu LC-2010C HT Instrument. Column Name: YMC TRIART-18 5u (250*4.6 mm) operating at ambient temperature and Flow rate of 1.0 ml/min or on Shimadzu LC-2010C HT Instrument. Column Name: YMC C18 5u (250*4.6 mm) operating at ambient temperature and Flow rate of 1.0 ml/min.

2-(4-Chlorophenyl)-3-methyl-1-{spiro[1,3-benzodioxole-2,4'-piperidine]-1'-yl}butan-1-one (2a; RS1): To a solution of 2-(4-chloro-phenyl)-3-methyl-butyric acid (1a, 0.5 g, 2.61 mmol) in THF (4 mL) was added spiro[1,3-benzodioxole-2,4'-piperidine] (0.66 g, 3.13 mmol), T3P (1.0 mL, 3.92 mmol) and Et3N (0.7 mL, 5.23 mmol) at rt. The reaction was stirred at rt for 16 h and then diluted with water (30 mL) and extracted with EtOAc (3 x 50 mL). The combined organic layer was washed with brine, dried over anhydrous Na2SO4 and evaporated under reduced pressure. Purification by column chromatography using silica gel (100-200 mesh) (20 % EtOAc in n-hexane) afforded 2a (0.4 g, 40 %) as a white solid. LC-MS: t_R 3.71 min, 100 % (265 nm); t_R 3.71 min, 100 % (220 nm). ^{1}H NMR (600 MHz, DMSO-d6): δ 7.34 – 7.48 (m, 4 H), 6.75 - 6.91 (m, 4 H), 3.73 - 3.82 (m, 2 H), 3.63 - 3.72 (m, 2 H), 3.55 - 3.63 (m, 1 H), 2.26 (dsept, J = 9.9, 6.6 Hz, 1 H), 1.77 - 1.90 (m, 2 H), 1.64 - 1.76 (m, 1 H), 1.31 - 1.41 (m, 1 H), 0.96 (J, d = 6.3 Hz, 3 H), 0.62 (d, J = 6.7 Hz, 3 H). ^{13}C NMR (150 MHz, DMSO-d^6): δ = 170.81, 146.22, 146.20, 138.45, 131.40, 130.00 (2C), 128.43 (2C), 121.47 (2C), 115.62, 108.70 (2C), 53.11, 42.26, 38.98, 35.05, 34.28, 31.69, 21.60, 19.81. HRMS ($C_{22}H_{24}ClNO_3$): calcd. 385.1445; found 385.1448.
LC/MS (Method A). t_R 9.01 min, 96.68 % (220 nm); MS calculated: 385.0, MS found: 386.0 (M+H, 1Cl).
HPLC PURITY: 98.56 % (λ210 nm); HPLC analysis was performed on Shimadzu LC-2010C HT Instrument using a YMC C18 5u (250*4.6 mm) column operated at ambient temperature and a flow rate of 1.0ml/min. The following scheme was applied: mobile phase from 90 % (10 mM NH_4OAc in water) and 10 % acetonitrile for 0.01min, mobile phase from 10 % (10 mM NH_4OAc in water) and 90 % acetonitrile for 7 min, held in this composition up to 20 min, then returned to initial composition in 21 min.
The two enantiomers of **2a** (100 mg) were separated on a Reprosil Chiral NR column (20 % EtOH in n-heptane) to give after precipitation from CH2Cl2 with n-pentane (-)-(S)-2a (40 mg, 40 %) and (+)-(R)-2a (38 mg, 38 %) as off-white solids. (-)-(2S)-2-(4-chlorophenyl)-3-methyl-1-spiro[1,3-benzodioxole-2,4'-piperidine]-1'-ylbutan-1-one ((-)-(S)-2a; S-RS1): LC-MS: t_R 3.71 min, 95.25 % (265 nm); t_R 3.71 min, 98.08 % (215 nm). α]^{20}D = -2.73 (c 1.0, $CHCl_3$); [α]^{20}365 = -29.88 (c 1.0, $CHCl_3$). ^{1}H NMR (600 MHz, DMSO-d_6): δ = 7.34 - 7.48 (m, 4 H), 6.73 - 6.95 (m, 4 H), 3.72 - 3.81 (m, 2 H), 3.63 - 3.71 (m, 2 H), 3.55 - 3.62 (m, 1 H), 2.25 (dsept, J = 9.8, 6.6 Hz, 1 H), 1.79 - 1.91 (m, 2 H), 1.65 - 1.76 (m, 1 H), 1.31- 1.40 (m, 1 H), 0.96 (d, J = 6.3 Hz, 3 H), 0.62 (d, J = 6.7 Hz, 3 H). ^{13}C NMR (150 MHz, DMSO-d_6): δ = 170.81, 146.20 (2C), 138.45, 131.40, 130.00 (2C), 128.43 (2C), 121.47 (2C), 115.62, 108.70 (2C), 53.11, 42.26, 38.98, 35.05, 34.28, 31.69, 21.60, 19.81. HRMS ($C_{22}H_{24}ClNO_3$): calcd. 385.1445; found 385.1446. Single crystals were formed at RT over time, suitable for X-ray crystallographic analysis. A single crystal was mounted in a loop and cooled to 130 K in a nitrogen stream. Data were collected on a Gemini R Ultra diffractometer (Rigaku) with Cu-K-alpha-radiation (1.54184 Å) and processed with the Crysalis-package. Structure solution and refinement was performed using the ShelXTL software (Bruker AXS, Karlsruhe) (SI Appendix, Table S4). (+)-(2R)-2-(4-chlorophenyl)-3-methyl-1-spiro[1,3-benzodioxole-2,4'-piperidine]-1'-ylbutan-1-one ((+)-(R)-2a; R-RS1): LC-MS: t_R 3.71 min, 99.99 % (265 nm); t_R 3.71 min, 10.00 % (215 nm). [α]^{20}D = +3.84 (c 1.0, $CHCl_3$); [α]^{20}365 = +31.26 (c 1.0, $CHCl_3$). ^{1}H NMR (600 MHz, DMSO-d_6): δ = 7.34 - 7.48 (m, 4 H), 6.73 - 6.95 (m, 4 H), 3.72 - 3.81 (m,

2 H), 3.63 - 3.71 (m, 2 H), 3.55 - 3.62 (m, 1 H), 2.25 (dsept, J = 9.8, 6.6 Hz, 1 H), 1.79 - 1.91 (m, 2 H), 1.65 - 1.76 (m, 1 H), 1.31- 1.40 (m, 1 H), 0.96 (d, J = 6.3 Hz, 3 H), 0.62 (d, J = 6.7 Hz, 3 H). ^{13}C NMR (150 MHz, DMSO-d_6): δ = 170.81, 146.20 (2C), 138.45, 131.40, 130.00 (2C), 128.43 (2C), 121.47 (2C), 115.62, 108.70 (2C), 53.11, 42.26, 38.98, 35.05, 34.28, 31.69, 21.60, 19.81. HRMS ($C_{22}H_{24}ClNO_3$): calcd. 385.1445; found 385.1446. Crystallization from ethanole by evaporation provided single crystals suitable for X-ray crystallographic analysis. A single crystal was mounted in a loop and cooled to 130 K in a nitrogen stream. Data were collected on a Gemini R Ultra diffractometer (Rigaku) with Cu-K-alpha-radiation (1.54184 Å) and processed with the Crysalis-package. Structure solution and refinement was performed using the ShelXTL software (Bruker AXS, Karlsruhe) (SI Appendix Table S4).

3-{1'-[2-(4-Chlorophenyl)-3-methylbutanoyl] spiro [1,3-benzodioxole-2,4'-piperidine]-6-yl}propanoic acid (2b; RS15)

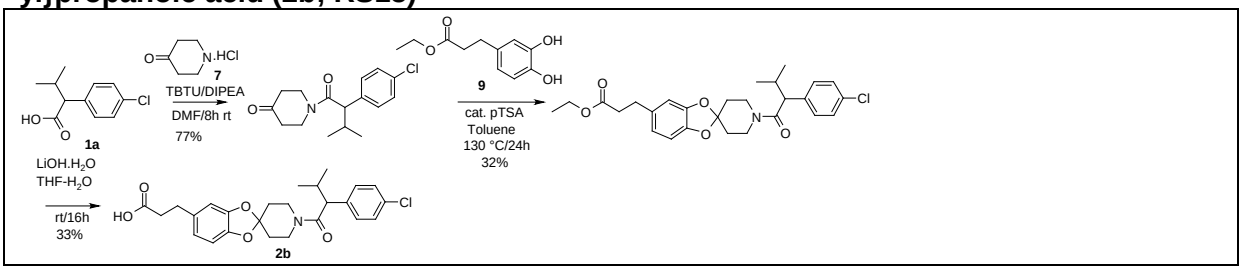

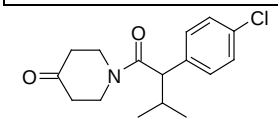

1-[2-(4-Chloro-phenyl)-3-methyl-butyryl]-piperidin-4-one: To a solution of 2-(4-chloro-phenyl)-3-methyl-butyric acid (**1a**, 0.5 g, 2.35 mmol) in DMF (8 mL) was added piperidin-4-one.HCl salt (0.38 g, 2.82 mmol), TBTU (1.1 g, 3.52 mmol) and DIPEA (1.6 g, 9.40 mmol) at rt. Reaction was stirred at rt for 8h and then diluted with water (30 mL) and extracted with EtOAc (3 X 30 mL). The combined organic layer was washed with brine (20 mL), dried over anhydrous Na_2SO_4 and evaporated under reduced pressure. Purification by combi flash (30 % EtOAc in n-hexane) afforded 1-[2-(4-chloro-phenyl)-3-methyl-butyryl]-piperidin-4-one (0.53 g, 77 %) as an off-white solid.
LC/MS (Method B). t_R 3.32 min, 94.17 % (220 nm); MS found: 294.1 (M+H, 1Cl).

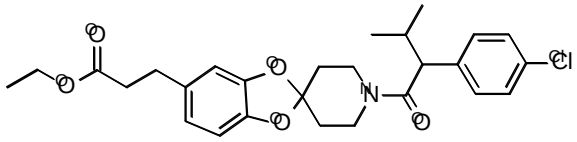

Ethyl 3-{1'-[2-(4-chlorophenyl)-3-methylbutanoyl]spiro[1,3-benzodioxole-2,4'-piperidine]-5-yl}propanoate: To a stirred solution of 1-[2-(4-chloro-phenyl)-3-methyl-butyryl]-piperidin-4-one (0.3 g, 1.02 mmol) and 3-(3, 4-dihydroxy-phenyl)-propionicacid ethyl ester (**9**) (0.21 g, 1.02 mmol) in toluene (20 mL) was added pTSA (0.029 g, 0.15 mmol). The resulting mixture was heated to reflux at 130 °C in Dean-Stark assembly for 24h and then evaporated under reduced pressure. Purification by column chromatography using silica gel (230-400 mesh; 20 % EtOAc in n-hexane) afforded ethyl 3-{1'-[2-(4-chlorophenyl)-3-ethylbutanoyl]spiro[1,3-benzodioxole-2,4'-piperidine]-5-yl}propanoate (0.16 g, 32 %) as a colourless oil.
LC/MS (Method B). t_R 3.46 min, 87.5 % (220 nm); MS found: 486.2 (M+H, 1Cl).

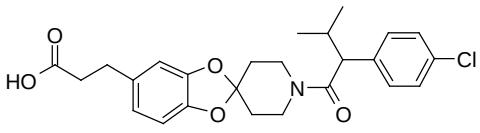

3-{1'-[2-(4-Chlorophenyl)-3-methylbutanoyl] spiro [1,3-benzodioxole-2,4'-piperidine]-6-yl}propanoic acid (2b; RS15): To a stirred solution of ethyl 3-{1'-[2-(4-chlorophenyl)-3-ethylbutanoyl]spiro[1,3-benzodioxole-2,4'-piperidine]-5-yl}propanoate (0.16 g, 0.32 mmol) in THF:H_2O (5:3 mL) was added LiOH.H_2O (0.035 g, 0.82 mmol) at rt. The resulting mixture was stirred at room temperature for 16h and then diluted with water, adjusted to PH 5-6 using saturated ammonium chloride solution and extracted with EtOAc (2 x 20 mL). The combined organic layer was dried over anhydrous Na_2SO_4 and concentrated under reduced pressure to obtaine crude compound which was purified by column chromatography (230-400 mesh silicagel; 1.5 % MeOH in DCM) to afford **2b** (0.05 g, 33 %) as an off-white solid. LC-MS: t_R 3.23 min, 99.52 % (265 nm); t_R 3.23 min, 98.75 % (220 nm). ^{1}H NMR (600 MHz, DMSO-d_6): δ 12.08 (br s, 1 H), 7.36 - 7.43 (m, 4 H), 6.69 - 6.78 (m, 2 H), 6.63 (br t, J = 6.1 Hz, 1 H), 3.54 - 3.79 (m, 5 H), 2.70 (q, J = 7.4 Hz, 2 H), 2.46 (q, J = 7.4 Hz, 2 H), 2.25 (dt, J = 9.9, 6.6 Hz, 1 H), 1.75 - 1.89 (m, 2 H), 1.62 - 1.73 (m, 1 H), 1.35 (dt, J = 8.6, 4.2 Hz, 1 H), 0.95 (d, J = 6.3 Hz, 3 H), 0.62 (d, J = 6.7 Hz, 3 H). ^{13}C NMR (150 MHz, DMSO-d_6): δ = 173.74, 170.80, 146.28, 144.55, 138.46, 134.44, 131.40, 130.00 (2C), 128.43 (2C), 120.81, 115.75, 108.80, 108.12, 53.10, 42.27, 38.98, 35.49, 35.09, 34.32, 31.69, 30.06, 21.60, 19.82. HRMS ($C_{25}H_{28}ClNO_5$): calcd. 457.1656; found 457.1656.
LC/MS (Method C). t_R 5.16 min, 98.8 % (220 nm); MS found: 458 (M+H, 1Cl).
HPLC PURITY: 97.88 % (λ205 nm); HPLC Analysis was carried out on Shimadzu LC-2010C HT Instrument. Column Name: YMC TRIART C18 5u (150*4.6 mm) operating at ambient temperature and Flow rate of 1.0ml/min. Mobile Phase: B-10 mM NH_4OAc in Water, A-Acetonitrile; Mobile Phase from 90 % (10 mM NH_4OAc in Water) and 10 % Acetonitrile for 0.01min, Mobile Phase from 20 % (10 mM NH_4OAc in Water) and 80 % Acetonitrile for 7.0 min, Mobile Phase from 10 % (10 mM NH4OAC in Water) and 90 % Acetonitrile for 20.0 min, then returned to initial composition in 21 min.

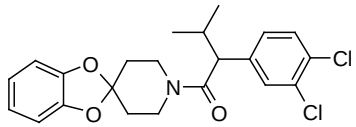

2-(3,4-Dichlorophenyl)-3-methyl-1-{spiro[1,3-benzodioxole-2,4'-piperidine]-1'-yl}butan-1-one (2c; RS11): To a solution of 2-(3,4-dichloro-phenyl)-3-methyl-butyric acid (**1c**, 0.2 g, 0.80 mmol) in DMF (4 mL) was added TBTU (0.39 g, 1.21 mmol) and DIPEA (0.2 g, 1.61 mmol) at rt and stirred for 20 min. and then treatded with spiro[1,3-benzodioxole-2,4'-piperidine] (0.18 g, 0.97 mmol). The reaction was stirred at room temperature for 8h and was then diluted with water (20 mL) and extracted with EtOAc (2 X 20 mL). The combined organic layer was washed with brine, dried over anhydrous Na_2SO_4 and evaporated under reduced pressure to afford 0.28 g crude compound which was purified by prep HPLC to afford **2c** (0.05 g, 15 %) as an off white solid. LC-MS: t_R 3.88 min, 100 % (265 nm); t_R 3.88 min, 100 % (220 nm). ^{1}H NMR (600 MHz, DMSO-d_6): δ 7.66 (d, J = 1.9 Hz, 1 H), 7.60 (d, J = 8.3 Hz, 1 H), 7.39 (dd, J = 8.3, 1.9 Hz, 1 H), 6.76 - 6.93 (m, 4 H), 3.79 - 3.90 (m, 2 H), 3.64 - 3.77 (m, 2 H), 3.55 - 3.62 (m, 1 H), 2.25 (dsept, J = 16.6, 6.5 Hz, 1 H), 1.82 - 1.92 (m, 2 H), 1.73 - 1.81 (m, 1 H), 1.47 - 1.62 (m, 1 H), 0.95 (d, J = 6.3 Hz, 3 H), 0.64 (d, J = 6.7 Hz, 3 H). ^{13}C NMR (150 MHz, DMSO-d_6): δ = 170.52, 146.25, 146.21, 140.65, 130.93, 130.62, 130.06, 129.46, 128.55, 121.49 (2C), 115.59, 108.73, 108.71 (2C), 52.42, 42.28, 35.19, 34.36, 31.96, 21.43, 19.76. HRMS ($C_{22}H_{23}Cl_2NO_3$): calcd. 419.1055; found 419.1062.

LC/MS (Method A). t_R 9.5 min, 100 % (220 nm); MS found: 420.1 (M+H, 2Cl).
HPLC PURITY: 99.68 % (λ210 nm); HPLC Analysis was carried out on Shimadzu LC-2010C HT Instrument. Column Name: Purosphere RP18 5u (250*4.6 mm) operating at ambient temperature and Flow rate of 1.0 ml/min. Mobile Phase: B-10 mM NH_4OAc in Water, A-Acetonitrile; Mobile Phase from 90 % (10 mM NH_4OAc in Water) and 10 % Acetonitrile for 0.01 min, Mobile Phase from 10 % (10 mM NH_4OAc in Water) and 90 % Acetonitrile for 7.0 min, held in this composition up to 20min, then returned to initial composition in 21 min.

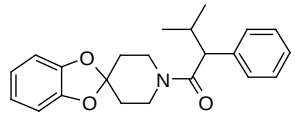

3-Methyl-2-phenyl-1-{spiro [1,3-benzodioxole-2,4'-piperidine]-1'-yl}butan-1-one (2d; **RS9):** To a solution of 3-methyl-2-phenyl-butyric acid (**1d**, 0.05 g, 0.28 mmol) in DMF (2 mL) was added spiro[1,3-benzodioxole-2,4'-piperidine] (0.053 g, 0.28 mmol), TBTU (0.13 g, 0.42 mmol) and DIPEA (0.072 g, 0.56 mmol) at rt. The resulting mixture was stirred at room temperature for 16h and was then diluted with water (10 mL) and extracted with EtOAc (3 X 10 mL). The combined organic layer was washed with brine, dried over anhydrous Na_2SO_4 and evaporated under reduced pressure. Purification by column chromatography (100-200 mesh silicagel; 20 % EtOAc in n-hexane) afforded **2d** (0.045 g, 46 %) as an white solid. LC-MS: t_R 3.52 min, 100 % (265 nm); t_R 3.52 min, 100 % (220 nm). ^{1}H NMR (600 MHz, DMSO-d_6): δ 7.30 - 7.37 (m, 4 H), 7.22 - 7.29 (m, 1 H), 6.82 - 6.88 (m, 1 H), 6.74 - 6.80 (m, 3 H), 3.63 - 3.80 (m, 4 H), 3.48 - 3.56 (m, 1 H), 2.28 (dquin, J = 9.8, 6.7, 6.7, 6.7, 6.7 Hz, 1 H), 1.81 - 1.89 (m, 1 H), 1.71 - 1.80 (m, 1 H), 1.59 - 1.69 (m, 1 H), 1.21 (dt, J = 13.4, 6.5 Hz, 1 H), 0.97 (d, J = 6.3 Hz, 3 H), 0.62 (d, J = 6.7 Hz, 3 H). ^{13}C NMR (150 MHz, DMSO-d_6): δ = 171.01, 146.21, 139.38, 128.47 (2C), 128.14 (2C), 126.78, 121.45 (2C), 115.66, 108.68 (2C), 54.17, 42.28, 38.95, 34.86, 34.24, 31.53, 21.76, 19.94. HRMS ($C_{22}H_{25}NO_3$): calcd. 351.1834; found 351.1851.
LC/MS (Method A). t_R 8.53 min, 87.9 % (220 nm); MS found: 352.0 (M+H).
HPLC PURITY: 98.95 % (λ210 nm); HPLC Analysis was carried out on Shimadzu LC-2010C HT Instrument. Column Name: X-Terra RP18 5u (250*4.6 mm) operating at ambient temperature and Flow rate of 1.0 ml/min. Mobile Phase: B-10 mM NH_4OAc in Water, A-Acetonitrile; Mobile Phase from 30 % (10 mM NH_4OAc in Water) and 70 % Acetonitrile for 0.01min, Mobile Phase from 10 % (10 mM NH_4OAc in Water) and 90 % Acetonitrile for 10 min, held in this composition up to 20 min, then returned to initial composition in 21 min.

2-(5-Chloro-6-hydroxypyridin-2-yl)-1-{spiro[1,3-benzodioxole-2,4'-piperidine]-1'-yl}ethan-1-one (2e; RS16)

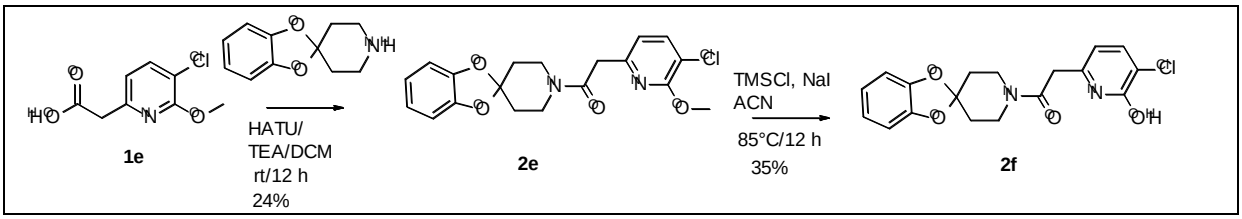

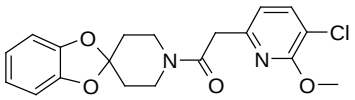

2-(5-Chloro-6-methoxypyridin-2-yl)-1-{spiro[1,3-benzodioxole-2,4'-piperidine]-1'-yl}ethan-1-one (2e): To a solution of 2-(5-chloro-6-methoxypyridin-2-yl) acetic acid (**1e**, 0.09 g, 0.44 mmol) in DCM (2 mL) was added HATU (0.20 g, 0.53 mmol) and TEA (0.09 mL, 0.67 mmol) at 0 °C. The reaction was stirred at rt for 30 min and then treated with spiro[1,3-benzodioxole-2,4'-piperidine] (0.08 g, 0.448 mmol). The reaction was further stirred for 12 h at room temperature. Water (5 mL) was then added and extracted with DCM (3 x 5 mL). The combined organic layer was dried over anhydrous Na_2SO_4 and evaporated under reduced pressure to provide crude mass (0.15 g) as yellow oil. Purification by column chromatography (100-200 mesh silicagel; 10-20 % EtOAc in n-hexane) afforded 2-(5-chloro-6-methoxypyridin-2-yl)-1-{spiro[1,3-benzodioxole-2,4'-piperidine]-1'-yl}ethan-1-one **2e** (0.04 g, 24 % yield) as an off white solid.
LC/MS (Method A). t_R 7.65 min, 94.68 % (220 nm); MS found: 375.1 (M+H, 1Cl).

HPLC PURITY: 95.43 % (λ210 nm); HPLC Analysis was carried out on Shimadzu LC-2010C HT Instrument. Column Name: YMC18 5u (250*4.6 mm) operating at ambient temperature and Flow rate of 1.0 ml/min. Mobile Phase: B-10 mM NH_4OAc in Water, A-Acetonitrile; Mobile Phase from 30 % (10 mM NH_4OAc in Water) and 70 % Acetonitrile for 0.01 min, Mobile Phase from 10 % (10 mM NH_4OAc in Water) and 90 % Acetonitrile for 7 min, held in this composition up to 20 min, then returned to initial composition in 21 min.

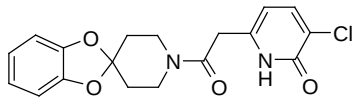

2-(5-Chloro-6-hydroxypyridin-2-yl)-1-{spiro[1,3-benzodioxole-2,4'-piperidine]-1'-yl}ethan-1-one (2f; RS16): To a solution of 2-(5-chloro-6- methoxypyridin-2-yl)-1-{spiro[1,3-benzodioxole-2,4'-piperidine]-1'-yl}ethan-1-one (**2e**, 0.06 g, 0.16 mmol) in acetonitrile (5.0 mL) was added NaI (0.07 g, 0.49 mmol) and TMSCl (0.05 g, 0.49 mmol). Reaction mixture was refluxed for 6 h and then evaporated under reduced pressure. The crude mass was quenched with saturated solution of sodium thio sulphate (10 mL) and extracted with EtOAc (2 x 10 mL). The combined organic layer was dried over anhydrous Na_2SO_4 and evaporated under reduced pressure. Purification by column chromatography (100-200 mesh silicagel; 20 % EtOAc in n-hexane) afforded **2f** (0.02 g, 35 % yield) as an off-white solid. LC-MS: t_R 2.16 min, 99.4 % (265 nm); t_R 2.16 min, 99.45 % (220 nm). ^{1}H NMR (600 MHz, DMSO-d_6): δ 12.01 (br s, 1 H), 7.65 (d, J = 7.4 Hz, 1 H), 6.90 (dd, J = 5.7, 3.3 Hz, 2 H), 6.83 (dd, J = 5.6, 3.3 Hz, 2 H), 6.06 (br d, J = 7.4 Hz, 1 H), 3.72 (s, 2 H), 3.60 - 3.69 (m, 4 H), 2.03 - 2.09 (m, 2 H), 1.90 -1.97 (m, 2 H). ^{13}C NMR (150 MHz, DMSO-d_6): δ = 166.57, 158.60, 146.32, 143.06, 138.98, 121.98, 121.50 (2C), 115.92, 108.74 (2C), 105.60, 42.41, 38.88, 36.51, 34.58, 34.16. HRMS ($C_{18}H_{17}N_2O_4$): calcd. 360.0877; found 360.0895.
LC/MS (Method A). t_R 5.56 min, 98.52 % (220 nm); MS found: 361.1 (M+H, 1Cl).
HPLC PURITY: 99.00 % (λ210 nm); HPLC Analysis was carried out on WATER-2998 Instrument. Column Name: YMC18 5u (250*4.6 mm) operating at ambient temperature and Flow rate of 1.0 ml/min. Mobile Phase: B-10 mM NH_4OAc in Water, A-Acetonitrile; Mobile Phase from 90 % (10 mM NH_4OAc in Water) and 10 % Acetonitrile for 0.01 min, Mobile Phase from 10 % (10 mM NH_4OAc in Water) and 90 % Acetonitrile for 10 min, held in this composition up to 20 min, then returned to initial composition in 21min.

Synthesis of 1g; RS13, 3; RS6, and 4; RS8:

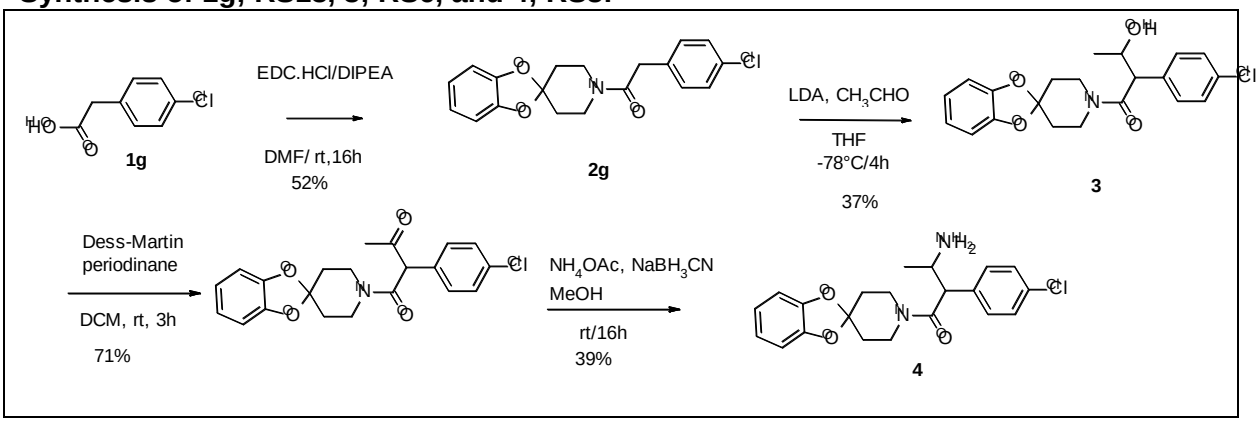

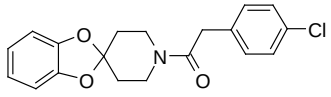

2-(4-chlorophenyl)-1-{spiro [1, 3-benzodioxole-2,4'-piperidine]-1'-yl}ethan-1-one (2g; RS13): To a solution of (4-Chloro-phenyl)-acetic acid (**1g**, 2.6 g, 15.69 mmol) in DMF (15 mL) was added DIPEA (5.4 ml, 31.38 mmol) and EDC.HCl (3.6 g, 23.53 mmol) at room temperature and stirred for 20 min. Then added spiro[1,3-benzodioxole-2,4'-piperidine] (3.0 g, 15.69 mmol) at room temperature. The resulting mixture was stirred at room temperature for 16h and then diluted with water (50 mL) and extracted with EtOAc (3 X 40 mL).

Combined organic layer was washed with brine (50 mL) dried over anhydrous Na_2SO_4 and evaporated under reduced pressure. Purification by column chromatography using silica gel (100-200 mesh; 15 % EtOAc in n-hexane) afforded **2g** (2.8 g, 52 %) as an off-white solid. LC-MS: t_R 3.12 min, 100 % (265 nm); t_R 3.12 min, 100 % (220 nm). ^{1}H NMR (600 MHz, DMSO-d_6): δ 7.38 (d, J = 8.4 Hz, 2 H), 7.27 (d, J = 8.4 Hz, 2 H), 6.87 - 6.90 (m, 2 H), 6.80 - 6.83 (m, 2 H), 3.79 (s, 2H), 3.64 - 3.67 (m, 2 H), 3.62 - 3.70 (m, 2 H), 1.87 - 1.92 (m, 4 H). ^{13}C NMR (150 MHz, DMSO-d_6): δ = 168.61, 146.30, 134.93, 131.04 (2C), 128.16 (2C), 121.46 (2C), 115.85, 108.71 (2C), 42.57, 40.05, 38.66, 38.57, 34.74, 34.14. HRMS ($C_{19}H_{18}ClNO_3$): calcd. 343.0975; found 343.0981.
LC/MS (Method A). t_R 7.8 min, 100 % (220 nm); MS found: 344 (M+H, 1Cl).
HPLC PURITY: 99.82 % (λ210 nm); HPLC Analysis was carried out on Shimadzu LC-2010C HT Instrument. Column Name: YMC TRIART C18 5u (250*4.6 mm) operating at ambient temperature and Flow rate of 1.0ml/min. Mobile Phase: B-10 mM NH_4OAc in Water, A-Acetonitrile; Mobile Phase from 25 % (10 mM NH_4OAc in Water) and 75 % Acetonitrile for 0.01 min, held in this composition up to 30 min.

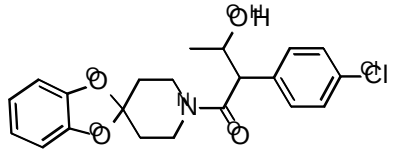

2-(4-chlorophenyl)-3-hydroxy-1-{spiro [1,3-benzodioxole-2,4'-piperidine]-1'-yl}butan-1-one (3; RS6): To a stirred solution of diispropyl amine (0.24 g, 2.39 mmol) in THF (5 mL) was added n-BuLi (2.6 M in THF) (0.9 mL, 2.39 mmol) at 0 °C and stirred for 10 min. The reaction was then cooled to -78 °C and treated with 2-(4-chlorophenyl)-1-{spiro [1, 3-benzodioxole-2,4'-piperidine]-1'-yl}ethan-1-one (**2f**, 0.4 g, 1.16 mmol) in THF (3 mL) drop wise. After 1h at -78 °C acetaldehyde (0.06 g, 1.39 mmol) in THF (1.0 mL) was added. After stirring at -78 °C for 2h the reaction was quenched with saturated ammonium chloride solution (10 mL) and extracted with EtOAc (3 x 20 mL). The combined organic layer was washed with brine, dried over anhydrous Na_2SO_4 and evaporated under reduced pressure. Purification by column chromatography using silica gel (230-400 mesh; 30 % EtOAc in n-hexane) afforded **3** (0.17 g, 37 % of ca 2:1 diastereomers) as a white solid. LC-MS: t_R 3.02 min, 76.7 % and 3.08 min, 22.5 % (265 nm); t_R 3.02 min, 63.3 % and 2.08 min, 36.0 % (215 nm). ^{1}H NMR (600 MHz, DMSO-d_6): δ 7.37 - 7.43 (m, 4 H), 6.76 - 6.90 (m, 4 H), 4.85 (d, J =, 5.1 Hz, 0.25 H), 4.56 (d, J=, 5.1 Hz, 0.75 H), 4.20 - 4.24 (m, 0.25 H), 4.08 - 4.12 (m, 0.75 H), 3.99 (d, J = 7.8 Hz, 0.25 H), 3.92 (d, J = 7.8 Hz, 0.75 H), 3.45 - 3.81 (m, 4 H), 1.70 – 1.94 (m, 3 H), 1.41 - 1.46 (m, 0.25H), 1.25 - 1.32 (m, 0.75H), 1.12 (d, J = 5.9 Hz, 2.25 H), 0.86 (d, J = 5.9 Hz, 0.75 H). ^{13}C NMR (150 MHz, DMSO-d_6, mojor diastereomer): δ = 170.53, 146.20 (2C), 136.93, 131.37, 130.70 (2C), 128.07 (2C), 121.48 (2C), 115.57, 108.71 (2C), 68.41, 53.71, 40.43 (2C), 34.78, 34.14, 22.18. HRMS (major diastereomer $C_{21}H_{22}ClNO_4$): calcd. 387.1237; found 387.1247; (minor diastereomer $C_{21}H_{22}ClNO_4$): calcd. 387.1237; found 387.1248.
LC/MS (Method B). t_R 12.98 min, 73.3 % and t_R 14.35 min, 26 % (220 nm); MS found: 388.0 and 388.3 (M+H, 1Cl).
HPLC PURITY: PEAK-I-76.88 %, PEAK-II-23.12 % (λ210 nm); HPLC Analysis was carried out on WATER 2998 Instrument. Column Name: X-bridge C18 5u (250*4.6 mm) operating at ambient temperature and Flow rate of 1.0 ml/min. Mobile Phase: B-10 mM NH_4OAc in Water, A-Acetonitrile; Mobile Phase from 45 % (10 mM NH_4OAc in Water) and 55 % Acetonitrile for 0.01 min, held in this composition up to 33 min,

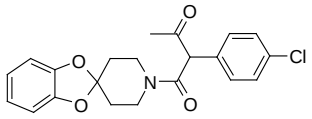

2-(4-Chlorophenyl)-1-{spiro [1,3-benzodioxole-2,4'-piperidine]-1'-yl}butane-1,3-dione: To a stirred solution of 2-(4-chlorophenyl)-3-hydroxy-1-{spiro [1,3-benzodioxole-2,4'-piperidine]-1'-yl}butan-1-one (**3**) (0.45 g, 1.16 mmol) in DCM (15 mL) was added Dess-

Martin periodinane (0.59 g, 1.39 mmol) portion wise at 0 °C. The resulting reaction mixture was stirred at room temperature for 3h and then filtered through celite and washed with DCM (2 x 20 mL). Filtrate was evaporated under reduced pressure and purified by column chromatography (230-400 mesh silicagel; 30 % EtOAc in n-hexane) to afford 2-(4-chlorophenyl)-1-{spiro [1,3-benzodioxole-2,4'-piperidine]-1'-yl}butane-1,3-dione (0.32 g, 71 %) as an off-white solid.
LC/MS (Method B). t_R 3.41 min, 97.4 % (220 nm); MS found: 385.9 (M+H, 1Cl).

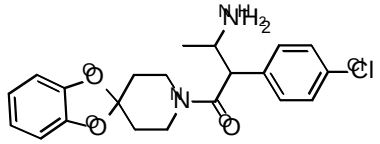

3-Amino-2-(4-chlorophenyl)-1-{spiro[1,3-benzodioxole-2,4'-piperidine]-1'-yl}butan-1-one (4; RS8): To a stirred solution of 2-(4-chlorophenyl)-1-{spiro [1,3-benzodioxole-2,4'-piperidine]-1'-yl}butane-1,3-dione (0.15 g, 0.52 mmol) in methanol (5 mL) was added $NaBH_3CN$ (0.03 g, 0.52 mmol) and NH_4OAc (0.4 g, 5.24 mmol) at 0 °C. The resulting mixture was stirred at room temperature for 16h. After completion, monitored by TLC, conc. aq. HCl was added dropwise to the solution until the pH of the mixture dropped below 4 and a white solid precipitated. Methanol was removed by vacuum, water was added to the residue and washed with DCM (25 mL). Then 6M aq NaOH was added to the aqueous layer to raise the pH to >12 and extracted with DCM (3 x 20 mL). The organic layer was dried over anhydrous Na_2SO_4 and evaporated under reduced pressure. Purification by column chromatography using silica gel (230-400 mesh; 10 % MeOH in DCM) afforded **4** (0.08 g, 39 % of ca 4:1 diastereomers) as an colour less liquid. LC-MS: t_R 1.90 min, 79.8 % and 2.02 min, 18.7 % (265 nm); t_R 1.90 min, 79.7 % and 2.02 min, 19.1 % (220 nm). ^{1}H NMR (600 MHz, DMSO-d_6): δ 7.35 - 7.47 (m, 4 H), 6.76 - 6.89 (m, 4 H), 3.95 (d, J = 7.5 Hz, 0.8 H), 3.87 (d, J = 7.5 Hz, 0.2 H), 3.37 -3.78 (m, 6 H), 1.78 - 1.96 (m, 3 H), 1.67 - 1.77 (m, 1 H), 1.25 - 1.32 (m, 1 H), 1.07 (d, J = 6.3 Hz, 2.4 H), 0.80 (d, J = 6.3 Hz, 0.6 H). ^{13}C NMR (150 MHz, DMSO-d_6, mojor diastereomer): δ = 170.33, 146.19, 135.92, 131.92, 130.67 (2C), 130.00, 128.68, 128.56 (2C), 121.48, 115.54 (2C), 108.71 (2C), 53.08, 49.60, 42.34, 38.78, 34.69, 34.15, 20.92. HRMS (major diastereomer $C_{21}H_{23}ClN_2O_3$): calcd. 386.1397; found 386.1411; (minor diastereomer $C_{21}H_{23}ClN_2O_3$): calcd. 386.1397; found 386.1407.
LC/MS (Method A). t_R 6.18 min, 81 % and t_R 6.50 min, 17.6 % (220 nm); MS found: 386.9 (M+H, 1Cl).
HPLC PURITY: PEAK-I 82.12 %, PEAK-II-17.03 % (λ210 nm); HPLC Analysis was carried out on Shimadzu LC-2010C HT Instrument. Column Name: Purospher star C18 5u (250*4.6 mm) operating at ambient temperature and Flow rate of 1.0 ml/min. Mobile Phase: B-10 mM NH_4OAc in Water, A-Acetonitrile; Mobile Phase from 55 % (10 mM NH_4OAc in Water) and 45 % Acetonitrile for 0.01min, held in this composition up to 30 min.

Crystal soaking, data collection and structure determination of S-RS1-bound opsin
Crystals were readily obtained using purified bovine opsin N2C/D282C incubated with 0.5-1 times w/w porcine brain polar lipid prior to vapor diffusion sitting or hanging drop crystallization (11). Crystals were grown over a reservoir solution containing 3.0 to 3.5 M ammonium sulfate, 0.1 M sodium acetate pH 5.75 - 6.0, and 10 % (w/v) trehalose using a 1:1 ratio of reservoir solution and protein in the crystallization drop. Crystals of bovine opsin N2C/D282C were typically grown for four days before soaking with 3.75 to 5 mM S-RS1 in reservoir solution. The soaks were incubated for 24 h prior to flash cooling of crystals with liquid nitrogen. Diffraction data was collected at 100 K on beamline X10SA at the Swiss Light Source (Villigen, Switzerland). Collected data sets were integrated using XDS and scaled using SADABS (Bruker) (17). High resolution limits were set based on I/σ(I) around 1.0 and CC1/2 > 0.2. All structures were solved by molecular replacement in Phaser with a rhodopsin search model (PDB ID 4J4Q) (18, 19). Iterative model building was done with Coot and fefinement rounds were executed in Phenix (20, 21). The compound was modeled into the closely fitting F_o-F_c electron density as the iterative model building of opsin

converged. More iterative model building rounds were performed with the compound to complete the structural model. The final structures were validated with Molprobity (30). Structure analysis was performed with MOE 2015.10 (Chemical Computing Group), Pymol, Consurf using all known verterbrate rhodopsin sequences from the SwissProt database (as of May, 2016) and Caver to analyze cavities in the dark state (PDB ID: 1GZM), the metaII state (PDB ID: 3PQR) and the S-RS1-opsin complex (22-25). Statistics of structure determination are listed in Supplementary Table 1. Coordinates and structure factors have been deposited in the Protein Data Bank under PDB IDs 6FK6 (S-RS01), 6FK7 (RS06), 6FK8 (RS08), 6FK9 (RS09), 6FKA (RS11), 6FKB (RS13), 6FKC (RS15) and 6FKD (RS16).

1. Hassan M, Brown RD, Varma-O'brien S, & Rogers D (2006) Cheminformatics analysis and learning in a data pipelining environment. *Molecular diversity* 10(3):283-299.
2. Garvey D (December 21, 2012) WO/2012/174064.
3. Garvey D, Larosa G, Greenwood J, & Frye L (December 15, 2011) WO2011155983 (A1).
4. Stahl M, Mauser H, Tsui M, & Taylor NR (2005) A robust clustering method for chemical structures. *Journal of medicinal chemistry* 48(13):4358-4366.
5. Hawkins PCD, Skillman AG, & Nicholls A (2007) Comparison of shape-matching and docking as virtual screening tools. *J Med Chem* 50(1):74-82.
6. Gerber PR & Muller K (1995) Mab, a Generally Applicable Molecular-Force Field for Structure Modeling in Medicinal Chemistry. *J Comput Aid Mol Des* 9(3):251-268.
7. Deupi X, *et al.* (2012) Stabilized G protein binding site in the structure of constitutively active metarhodopsin-II. *Proceedings of the National Academy of Sciences of the United States of America* 109(1):119-124.
8. Jones G, Willett P, Glen RC, Leach AR, & Taylor R (1997) Development and validation of a genetic algorithm for flexible docking. *Journal of molecular biology* 267(3):727-748.
9. Jones G, Willett P, & Glen RC (1995) Molecular Recognition of Receptor-Sites Using a Genetic Algorithm with a Description of Desolvation. *Journal of molecular biology* 245(1):43-53.
10. Li J, Edwards PC, Burghammer M, Villa C, & Schertler GF (2004) Structure of bovine rhodopsin in a trigonal crystal form. *Journal of molecular biology* 343(5):1409-1438.
11. Mattle D, Singhal A, Schmid G, Dawson R, & Standfuss J (2015) Mammalian expression, purification, and crystallization of rhodopsin variants. *Methods in molecular biology* 1271:39-54.
12. Xie G, *et al.* (2011) Preparation of an activated rhodopsin/transducin complex using a constitutively active mutant of rhodopsin. *Biochemistry* 50(47):10399-10407.
13. Standfuss J, *et al.* (2007) Crystal structure of a thermally stable rhodopsin mutant. *Journal of molecular biology* 372(5):1179-1188.
14. Reeves PJ, Kim JM, & Khorana HG (2002) Structure and function in rhodopsin: a tetracycline-inducible system in stable mammalian cell lines for high-level expression of opsin mutants. *Proceedings of the National Academy of Sciences of the United States of America* 99(21):13413-13418.
15. Reeves PJ, Callewaert N, Contreras R, & Khorana HG (2002) Structure and function in rhodopsin: high-level expression of rhodopsin with restricted and homogeneous N-glycosylation by a tetracycline-inducible N-acetylglucosaminyltransferase I-negative HEK293S stable mammalian cell line. *Proceedings of the National Academy of Sciences of the United States of America* 99(21):13419-13424.
16. Singhal A, *et al.* (2013) Insights into congenital stationary night blindness based on the structure of G90D rhodopsin. *Embo Rep* 14(6):520-526.
17. Kabsch W (2010) Xds. *Acta Crystallogr D* 66:125-132.
18. Mccoy AJ, *et al.* (2007) Phaser crystallographic software. *J Appl Crystallogr* 40:658-674.
19. Park JH, *et al.* (2013) Opsin, a Structural Model for Olfactory Receptors? *Angew Chem Int Edit* 52(42):11021-11024.

20. nEmsley P & Cowtan K (2004) Coot: model-building tools for molecular graphics. *Acta Crystallogr D* 60:2126-2132.
21. Adams PD, *et al.* (2010) PHENIX: a comprehensive Python-based system for macromolecular structure solution. *Acta Crystallogr D* 66:213-221.
22. Landau M, *et al.* (2005) ConSurf 2005: the projection of evolutionary conservation scores of residues on protein structures. *Nucleic Acids Res* 33:W299-W302.
23. Glaser F, *et al.* (2003) ConSurf: identification of functional regions in proteins by surface-mapping of phylogenetic information. *Bioinformatics* 19(1):163-164.
24. DeLano WL (2009) PyMOL molecular viewer: Updates and refinements. *Abstr Pap Am Chem S* 238.
25. Choe HW, *et al.* (2011) Crystal structure of metarhodopsin II. *Nature* 471(7340):651-655.
26. Alexandrov AI, Mileni M, Chien EYT, Hanson MA, & Stevens RC (2008) Microscale fluorescent thermal stability assay for membrane proteins. *Structure* 16(3):351-359.
27. Stevens RC, Sancho J, & Martinez A (2010) Rescue of misfolded proteins and stabilization by small molecules. *Methods in molecular biology* 648:313-324.
28. Hattori M, Hibbs RE, & Gouaux E (2012) A Fluorescence-Detection Size-Exclusion Chromatography-Based Thermostability Assay for Membrane Protein Precrystallization Screening. *Structure* 20(8):1293-1299.
29. Chen Y, *et al.* (2015) A high-throughput drug screening strategy for detecting rhodopsin P23H mutant rescue and degradation. *Investigative ophthalmology & visual science*.
30. Chen VB, *et al.* (2010) MolProbity: all-atom structure validation for macromolecular crystallography. *Acta Crystallogr D* 66:12-21.